

# X-ray-diffraction determination of the Ni-dopant site in single-crystal $\text{YBa}_2\text{Cu}_3\text{O}_{7-\delta}$

S. A. Hoffman,\* M. A. Castro, G. C. Follis, and S. M. Durbin

*Department of Physics, Purdue University, West Lafayette, Indiana 47907-1396*

(Received 31 March 1993; revised manuscript received 1 November 1993)

Anomalous dispersive x-ray-diffraction measurements have determined the dopant-site distribution in Ni-doped single crystals of the high-temperature superconductor  $\text{YBa}_2\text{Cu}_3\text{O}_{7-\delta}$ . The data from a  $\text{YBa}_2[\text{Cu}_{0.83}\text{Ni}_{0.17}]_3\text{O}_{7-\delta}$  crystal show that over 95% of the Ni dopants occupy the Cu(2) site in the copper oxide planes, with negligible occupation of the Cu(1) copper oxide chain sites. General guidelines are presented for selecting the most effective  $hkl$  diffraction planes for measuring dopant concentration profiles. Direct measurement of the energy dependence of the dopant atomic scattering factors is also demonstrated.

## I. INTRODUCTION

Many modern materials contain dilute constituents which are important for understanding or controlling critical physical properties. Semiconductor dopants are a prime example, but dilute constituents are also crucial for various catalysts, metal alloys, ceramics, etc. In this analysis we are specifically motivated by an interest in low concentrations of Ni incorporated into the high-temperature oxide superconductor  $\text{YBa}_2\text{Cu}_3\text{O}_{7-\delta}$  as a probe of how magnetic moments perturb the superconducting state.

Interpreting dopant-induced changes in the high-temperature superconductors is one of the strategies available for investigating the still-elusive nature of this apparently new mechanism for superconductivity.<sup>1-4</sup> One complication with  $\text{YBa}_2\text{Cu}_3\text{O}_{7-\delta}$  is the presence of two inequivalent Cu sites in the unit cell, the Cu(1) copper oxide chain site and the two equivalent Cu(2) copper oxide plane sites, which are understood to play quite different roles with respect to superconductivity.<sup>5</sup> Meaningful analysis of dopant-induced behavior therefore requires a determination of the dopant-site distribution.

The need for more accurate determinations is clear from the literature, which is rife with conflicting results. Different x-ray and neutron studies of Zn dopants in the 1:2:3 superconductor, for example, have found that Zn resides preferentially in the chains,<sup>6</sup> in the planes,<sup>5,7</sup> or in both sites equally.<sup>8,9</sup> Various other "direct" determinations have relied on inferences from such parameters as Hall coefficients, oxygen uptake rates, and dopant-host nearest neighbor separations. Although there are many experimental techniques which may shed some light on dopant-site distributions, we decided that anomalous dispersive x-ray diffraction was most promising, and our results with a Ni-doped single crystal are described below. An early study which first utilized anomalous dispersive x-ray diffraction with these systems was conducted by Howland *et al.*<sup>8</sup> Their results for a Ni-doped powder specimen are not in agreement with ours. As we discuss later, this could be a genuine consequence of differing growth processes, or the result of recent improvements in the measuring technique.

## II. ANOMALOUS DISPERSIVE X-RAY DIFFRACTION

Crystallography's task of determining the precise location of all atoms within the unit cell of an unknown structure largely centers on the well-known phase problem in diffraction: While the amplitudes of the diffracted waves depend directly on the positions of the atoms, the detected beam intensities are proportional to the square of these amplitudes and hence some of the structural information is necessarily lost.<sup>10</sup> Simple structures can still be determined by comparing the set of measured diffracted beam intensities to calculated results from various hypothetical structures. The remarkable success of modern crystallography in solving large and highly complex structures is due in part to refined strategies for handling this phase problem, e.g., the isomorphous substitution and multiple anomalous dispersion techniques.<sup>11,12</sup> Equally important has been the availability of high-brightness x-ray synchrotron radiation sources.

In principle one could address the issue of dilute constituents by treating the entire system as an unknown structure and applying standard crystallographic techniques. At dilution, however, the particular constituent would only weakly perturb the intensities of the diffracted beams, and so one would like to make use of the known host structure as a kind of reference frame. This is the essence of the x-ray standing wave technique, for example, which takes advantage of the dynamical nature of diffraction from nearly perfect crystals and the sensitivity of secondary yield detection to permit site determinations for very low dopant concentrations.<sup>13-15</sup> The interference of the incident and diffracted waves produces a standing wave field, whose periodicity is that of the  $hkl$  Fourier component of the generalized scattering density function

$$\rho_{hkl}(\mathbf{r}, E) = \frac{1}{V} F_{hkl}(E) \exp(-2\pi i \mathbf{H}_{hkl} \cdot \mathbf{r}), \quad (1)$$

where  $\mathbf{H}_{hkl} = h\mathbf{b}_1 + k\mathbf{b}_2 + l\mathbf{b}_3$ , and the  $\mathbf{b}_i$  are the reciprocal lattice vectors. (This function differs from the true electron density function only by the energy dependence of the complex structure factor  $F_{hkl}$ .) By analogy with

the  $hkl$  atomic planes being found at maxima of the  $hkl$  Fourier components of the electron density, the maxima of the scattering function  $\text{Re}[\rho_{hkl}(\mathbf{r}, E)]$  are called the diffraction planes.<sup>16</sup> When x rays diffract from a perfect crystal, the physical reference system consists of these periodic diffraction planes, which are a function of both the unit cell structure and the atomic scattering factors (see Fig. 1).

We now consider the case where the concentration of the dopant is again too small for standard crystallographic techniques to work, e.g., fewer than one atom per unit cell, yet still large enough to produce a measurable difference in some diffracted beam intensities. This of course depends on the signal to noise ratio of the measurements, and hence this problem is better suited to a high-intensity synchrotron radiation source than standard laboratory x-ray sources. Realistic concentration limits will be discussed below. What makes the synchrotron radiation source essential, however, is the ability to continuously vary the energy of the x rays. One can then take advantage of the energy dependence of the dilute constituent's atomic scattering factor to obtain crystallographic phases, i.e., the well-known anomalous dispersion method.<sup>11,17</sup>

For a crystal containing a dilute constituent, we write the structure factor as

$$F_{hkl}(E) = \sum_n g_n(E) \exp(2\pi i \mathbf{H}_{hkl} \cdot \mathbf{r}_n), \quad (2)$$

where the summation is over all atom sites in the unit cell,  $\mathbf{r}_n$  is the displacement of the  $n$ th site from the origin, and  $\mathbf{H}_{hkl}$  is the reciprocal lattice vector of the reflection. For all sites which contain no dopants, the  $g_n$  are just the standard atomic scattering factors  $f_n$ . For sites partially occupied by dopants, we have

$$g_n(E) = a_{n,1} f_1(E) + a_{n,2} f_2(E), \quad (3)$$

where  $a_{n,1}$  and  $a_{n,2}$  are the occupation probabilities in site  $n$  for the atoms with scattering factors  $f_1(E)$  and  $f_2(E)$ , respectively. In our specific example, we need to determine the occupation probabilities  $a_{n,\text{Ni}}$  and  $a_{n,\text{Cu}}$  for the Cu(1) chain site and the two equivalent Cu(2) plane sites.

Included in the atomic scattering factors  $f_n$  are the Debye-Waller factors and the form factor dependence, which we do not write explicitly. The crucial energy dependence of the atomic scattering factors  $f_n$  is seen by writing in the usual way<sup>18</sup>

$$f(E) = f_0 + f'(E) + i f''(E), \quad (4)$$

where  $f_0$  is the high-energy limit corresponding to the number of electrons on the ion,  $f'$  is the dispersive part of the elastic scattering due to the photon's resonant interaction with each of the ion's bound electrons, and  $f''$  models the loss of scattered wave amplitude from photoelectric absorption of the incident photon. The anomalous terms  $f'$  and  $f''$  vary dramatically within 100 V or so of the  $K$  absorption edge, for example, but far from edges the atomic scattering factor is smooth and slowly varying.

From Eqs. (2)–(4) one sees that the square of the structure factor  $|F_{hkl}|^2$  and hence the intensity  $I_{hkl}$  will depend on the energy. Further, it is possible for a very small concentration  $a_n$  of dopant at position  $\mathbf{r}_n$  and an appropriate  $hkl$  reflection to produce a large fractional change in  $|F_{hkl}|^2$  as the energy is scanned through a dopant absorption edge. This is especially probable if the summation in Eq. (2) consists of terms of opposite signs which nearly cancel each other, i.e., a weak reflection. To further have good selectivity between sites  $\mathbf{r}_1$  and  $\mathbf{r}_2$ , these two positions should contribute terms to Eq. (2) having opposite signs. The effect of such a structure factor upon the scattering density function  $\rho_{hkl}(\mathbf{r}, E)$  is illustrated in Fig. 1.

For the site distribution of a dilute constituent to be determined, the intensity from one or more  $hkl$  reflections is measured as a function of x-ray energy across an absorption edge. These measurements can then be compared to calculations of  $|F_{hkl}|^2$ , in which the dopant distribution is treated as a fit parameter. An important simplification arises from having a set of measured intensities as a function of energy, since it is the relative

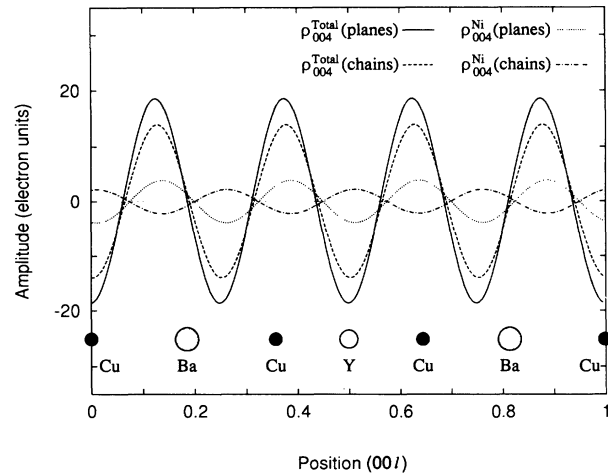


FIG. 1. The dependence of the 004 Fourier component of the scattering density function  $\rho(\mathbf{r}, E)$  on the Ni-dopant-site preference in a unit cell of  $\text{YBa}_2[\text{Cu}_{0.83}\text{Ni}_{0.17}]_3\text{O}_{7-\delta}$ . The largest sine wave (solid line) is the real part of  $\rho_{004}^{\text{total}}(\mathbf{r}, E)$  (see text) plotted against the  $c$ -axis coordinate, assuming all of the Ni dopants reside in Cu planes sites and with x rays at exactly the Ni  $K$  absorption edge energy. The large dashed-line sine curve is the corresponding  $\text{Re}[\rho_{004}^{\text{total}}(\mathbf{r}, E)]$  for Ni ions located in the Cu chain sites. The smaller dotted-line sine curve is the contribution from just the Ni ions to the generalized density function, i.e.,  $\text{Re}[\rho_{004}^{\text{Ni}}(\mathbf{r}, E)]$ , for Ni ions in the planes, and the dot-dashed sine curve is the contribution from these Ni ions in the chain sites. Also shown is the projection onto the  $c$  axis of the positions of the host structure metal ions. Note that the Cu chain site is essentially out of phase with the two Cu planes sites, and that the contributions from the Ni ions in the chains and planes have opposite signs. Also note that the relatively small amplitude (less than 20 electrons per unit cell) indicates that the 004 is a rather weak reflection, an important factor for having good sensitivity to low dopant concentrations.

change of intensity which can be compared to the calculations, obviating the need for converting measurements into absolute structure factor values.

We have developed a systematic procedure for selecting the most sensitive  $hkl$  reflections for determining the dopant's concentration profile, to supplement the general guidelines already mentioned. We numerically evaluate the derivative of the square of the structure factor with respect to the dilute constituent's concentration:

$$D_{hkl}(E, a_n) = \partial[|F_{hkl}(E, a_n)|^2]/\partial a_n. \quad (5)$$

For example, consider the problem of determining the Ni-site distribution between the two inequivalent sites in the 1:2:3 superconductor. In Table I we list the  $|F_{hkl}|^2$  and their derivatives with respect to the Ni concentration for 5% of all Cu atoms replaced by Ni. Two cases are considered: (1) having all of the Ni in the Cu(1) sites, and (2) having all Ni distributed equally between the two Cu(2) sites. The following calculations use an x-ray energy at the Ni  $K$  absorption edge (8333 keV), and were repeated for the  $(00l)$  reflections with  $l = 1, \dots, 9$ . Notice that whenever  $|F_{hkl}|^2$  is large, the relative sensitivity to the Ni concentration is quite small, as expected. In addition to wanting the magnitude of  $D_{hkl}(E, a_n)$  to be as large as possible, however, the response of the two different inequivalent sites should have opposite signs. One might then determine which of the two inequivalent sites has the greater occupation merely by observing whether the raw data generally increase or decrease in the vicinity of the absorption edge. Using this criterion and the magnitudes of the  $D_{00l}(E, a_n)$ , the most favorable reflection would be the 001, followed in order by 004, 002, and 007.

For general calculations we use atomic scattering fac-

TABLE I. Presented are calculations for  $\text{YBa}_2[\text{Cu}_{0.95}\text{Ni}_{0.05}]_3\text{O}_{7-\delta}$  indicating the sensitivities of a set of  $00l$  reflections to the presence of Ni in each of the two inequivalent Cu sites, for x rays at the Ni  $K$  absorption edge,  $E = 8333$  eV. For each reflection the square of the structure factor is given as a measure of the strength of the reflection. The sensitivity factor is  $D_{hkl}(E, a_n) = \partial[|F_{hkl}(E, a_n)|^2]/\partial a_n$ , i.e., the derivative of the intensity with respect to the Ni occupation factors. Both  $|F_{hkl}|^2$  and  $D_{hkl}$  are calculated for Ni in the Cu(1) chain and the Cu(2) plane sites. The criteria for optimal site selectivity with anomalous dispersion are (1) large  $D_{hkl}$ 's with opposite signs for the two sites and (2) a weak reflection. The optimal reflections are thus the 001, 004, 002, and 007, in descending order.

$hkl$	Cu(1) chains		Cu(2) planes	
	$ F_{hkl} ^2$	$D_{hkl}$	$ F_{hkl} ^2$	$D_{hkl}$
001	78.0	+0.64	59.0	-0.89
002	294.0	+0.22	277.0	-0.10
003	2423.0	+0.09	2457.0	+0.17
004	303.0	+0.31	257.0	-0.59
005	10 950.0	-0.05	11 014.0	-0.02
006	29 568.0	-0.03	29 513.0	-0.04
007	6125.0	+0.07	5903.0	-0.14
008	524.0	-0.24	522.0	-0.27
009	5271.0	+0.07	5245.0	+0.04

tors  $f_n(E)$  appropriate for isolated atoms.<sup>19</sup> For real materials, of course, the ideal resonance behavior of  $f'(E)$  and  $f''(E)$  can be substantially modified by the local chemical environment to produce so-called near-edge and extended x-ray-absorption fine-structure (EXAFS) phenomena.<sup>20</sup> A dopant with a strong "white line" character to  $f''(E)$  might result in rather complex behavior of the diffracted intensities near the absorption edge, making comparisons to calculations based on atomic scattering factors from isolated atoms invalid. For an experiment which intends to measure diffracted beam intensities as a function of energy near an absorption edge, however, an ideal solution is available: By measuring the fluorescence from the dilute constituent with the same specimen over the same energy range, one has a nearly direct measure of  $f_n''(E)$ . By adding appropriate analytic continuations far from the absorption edge one can generate the corresponding  $f_n'(E)$  via the standard Kramers-Kronig transformation.<sup>21-23</sup> These experimentally determined values of  $f_n(E)$  can then be used in the structure factor calculations, and to a good approximation the local chemical perturbations to the atomic scattering factors near the absorption edge will be properly accounted for.

Such an anomalous dispersion x-ray-diffraction measurement has been performed on a Ni-doped 1:2:3 superconductor crystal. This specimen contained 17% Ni, i.e.,  $\text{YBa}_2[\text{Cu}_{0.83}\text{Ni}_{0.17}]_3\text{O}_{7-\delta}$ . Although the specimen was a thin platelet only 0.5 mm by 0.5 mm, the data obtained at the National Synchrotron Light Source (beam line X-18a) from such crystals had better signal to background ratios than data from bulk polycrystalline samples. This crystal was prepared by standard flux-growth procedures,<sup>7</sup> except that 10% of the CuO was replaced by NiO. The Ni concentration for this particular specimen was determined by comparing its Ni and Cu  $K$  fluorescence yields with those from specially prepared polycrystalline standards. The Ni concentration was found to vary substantially among crystals taken from the same crucible.

Integrated intensities were obtained from sets of rocking curves which mapped out the two-dimensional angular range of reflection for a given reciprocal lattice vector  $\mathbf{H}_{hkl}$ . These are converted to  $|F_{hkl}|^2$  by correcting for absorption and geometrical effects, and the results for the 004 reflection are plotted versus x-ray energy in Fig. 2.

The function  $f''(E)$  was derived from a measurement of the Ni fluorescence yield from this specimen as the incident x-ray beam was scanned in energy through the absorption edge [using an energy-dispersive Si(Li) detector]. These data were corrected for absorption to produce a relative  $f''(E)$ , which was then put on an absolute basis by adjusting the asymptotic limits to match the theoretical values. The  $f''(E)$  are numerically inverted via a Kramers-Kronig transformation to produce the corresponding  $f'(E)$ ; we followed the procedure given by Cromer and Lieberman.<sup>22,23</sup> Note that our  $f'(E)$  and  $f''(E)$  are experimentally determined from the same specimen employed for the structure factor measurements. With the dopant  $f_n(E)$  determined, only the  $a_n$  remain as the fitting parameters describing the site occupancy of the Ni ions between the two inequivalent

Cu positions. Hence we can generate a curve for  $|F_H|^2$  versus energy for a particular distribution of Ni ions. The solid line in Fig. 2 corresponds to having all of the Ni in the CuO planes; the good agreement between the data and the calculated curve is lost if only 5% of the Ni ions are moved to the chain site in the calculation. From this analysis we conclude that Ni ions have a very strong preference for the Cu(2) planes.

Notice the remarkable sensitivity of this reflection to the x-ray energy near the Ni *K* absorption edge: The intensity decreases by nearly 30%. Also note that if all of the Ni atoms were located in the Cu(1) chain site, then the calculated intensity would instead increase by nearly 30%, a 60% difference in intensity between the two Ni sites. In this specimen approximately one out of six Cu atoms was replaced by a Ni atom, but this is only one out of every 26 atoms altogether. A more revealing measure is that all of the intensity change is caused by the resonant interaction with the two *K* shell electrons on the Ni atoms. These are two out of every 294 electrons in the crystal, or 0.68%. Of greater importance,

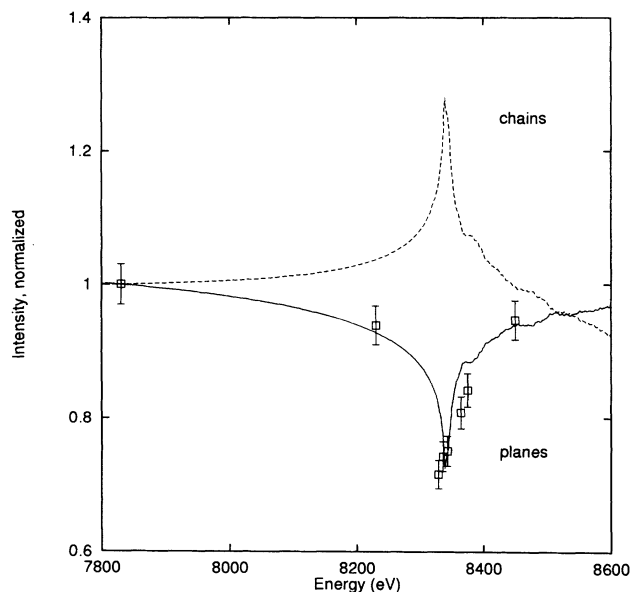


FIG. 2. Measured 004 intensities as a function of energy near the Ni *K* absorption edge for a  $\text{YBa}_2[\text{Cu}_{0.83}\text{Ni}_{0.17}]_3\text{O}_{7-\delta}$  single crystal. The intensities have been corrected for geometrical and absorption effects to make them proportional to the structure factor squared  $|F_{004}|^2$ , and these were normalized to make the lowest-energy data point unity. The solid line is a calculated fit in which all of the Ni atoms are located in the Cu(2) planes sites. Input data for the Ni atomic scattering factors  $f'(E)$  and  $f''(E)$  were derived from measurements of the Ni fluorescence yield versus energy from this same specimen (see text). A similar calculation with Ni in the Cu(1) chain sites produces a curve which is nearly the mirror image of this one, with all intensities increasing near the Ni absorption edge. The calculation assumes the free atom value for the Ni *K* absorption edge energy; the data indicate a small chemical shift in the true absorption edge.

however, is that the results shown in Fig. 2 suggest that with improved but still realistic signal to noise ratios, data with only a 1% change could have been measured. This would correspond to a Ni-site determination with a dopant concentration of only 0.5% of the Cu atoms.

### III. DISCUSSION

The anomalous dispersion data clearly resolve the question of Ni-site occupancy. The dramatic resonant behavior of the 004 diffracted intensity is an unambiguous demonstration of the Cu(2)-plane-site preference, with no more than 5% of the Ni ions present in the Cu(1) chains. This uncertainty in the minority site could readily be reduced by improved statistics in future measurements.

As already noted, the earlier study of Howland *et al.*<sup>8</sup> using anomalous dispersive x-ray diffraction to determine the Ni dopant site in  $\text{YBa}_2\text{Cu}_3\text{O}_{7-\delta}$  powder specimens concluded that there was no site preference between the two sites, a result apparently contradicted by the present work. One possible explanation is that the true site occupation is different for polycrystalline and single-crystalline materials. Neither the sintering of powders nor the flux growth of single crystals corresponds exactly to a true thermodynamic equilibrium of Ni-doped  $\text{YBa}_2\text{Cu}_3\text{O}_{7-\delta}$ ; hence the dopant distribution need not be identical.

Differences in measurement technique, however, may also account for the absence of site preference found with the powder specimens. We note three important differences from the earlier work.

(1) With a single-crystal specimen, it is possible to measure the complete integrated intensity of a given reflection, and with better separation of the true signal from other background scattering processes. A small resonant change in the diffracted intensity can be easily obscured by a background signal. Our own preliminary measurements on large, pressed pellets of doped  $\text{YBa}_2\text{Cu}_3\text{O}_{7-\delta}$  powders had signal to noise ratios inferior to the data from very small single-crystal specimens.

(2) The fits to the single-crystal data were obtained with the measured values of  $f_n(E)$  obtained from the diffraction specimen, instead of using the tabulated dispersion corrections for isolated atoms. The calculated fits hence include the local chemical perturbations to the scattering factor near the absorption edge.

(3) A larger number of data points for the single crystal were obtained in the immediate vicinity of the absorption edge, where the resonant behavior is most pronounced.

These results show that quantitative dopant-site distributions can be readily obtained from single crystals when using the high brightness and energy tunability of a synchrotron radiation source. Mosaic crystals are quite suitable, and even polycrystalline specimens can in principle be employed, although with a likely decrease in sensitivity due to reduced signal to noise ratios. For the particular example of  $\text{YBa}_2\text{Cu}_3\text{O}_{7-\delta}$ , dopant concentration levels down to 1% of the Cu content should produce good site determinations. As with all such x-ray determinations, the dopant atom must have an electron binding

energy large enough to interact with the diffracting x rays. Atoms with atomic numbers less than titanium's ( $Z = 22$ ,  $K$  shell binding energy = 4966 eV) would be considerably more difficult with this method.

The anomalous dispersion x-ray technique has certain advantages as an analytical tool. One measures only the diffracted x-ray beam, with no need to also detect secondary yields, as is the case with x-ray standing waves. Crystals of high quality are not required, since it is necessary only to measure a signal proportional to the square of the structure factor. This is easily done even with polycrystalline powder specimens, although good single crystals are preferred since the total reflecting power can be determined by measuring over a small range of angles, reducing unwanted background contributions. The drawback, of course, is that the dopant concentration must be high enough to measurably perturb the total diffracted beam intensity when the x rays resonantly interact with the dopant's bound electrons. The lowest detectible concentration is therefore strongly dependent on the accuracy with which diffracted beam intensities can be measured, and hence on the reliability and reproducibility of the diffractometer and the synchrotron radiation source itself. In the example studied here, Ni-doped  $\text{YBa}_2\text{Cu}_3\text{O}_{7-\delta}$ , the results suggest that achievable lower limits range from 0.1% to 1.0% of the overall atomic content.

#### IV. CONCLUSIONS

The experimental results presented here show that quantitative determination of dopant-site distributions using anomalous dispersive x-ray diffraction are feasible for concentrations which are already low enough to be relevant to current materials problems. This will certainly improve as the newest generation of x-ray synchrotron radiation sources become available. Because of the relative simplicity of the measurements and the ensuing analysis, such x-ray-diffraction determinations should provide a useful complement to x-ray absorption and other analytical techniques.

#### ACKNOWLEDGMENTS

The anomalous dispersion measurements at the Brookhaven National Synchrotron Light Source were greatly assisted by Dr. Steven Ehrlich at beam line X-18a, supported by the Department of Energy Grant No. DE-FG02-85ER45183. This research was supported by National Science Foundation Grant Nos. DMR 86-57587 and DMR 87-03993, the Indiana Center for Innovative Superconducting Technology, and the Kodak Foundation. One of the authors (S.M.D.) also wishes to thank the Hamburger Synchrotronstrahlungslabor (HASYLAB) for their hospitality while this manuscript was in preparation.

\*Present address: Cornell High Energy Synchrotron Source, Wilson Laboratory, Cornell University, Ithaca, NY 14853.

<sup>1</sup>S. A. Hoffman, M. A. Castro, G. C. Follis, and S. M. Durbin, *Physica C* **208**, 59 (1993).

<sup>2</sup>F. Nakamura, Y. Ochiiai, H. Shimizu, and Y. Narahara, *Phys. Rev. B* **42**, 2558 (1990).

<sup>3</sup>C. L. Seaman, J. J. Neumeier, M. B. Maple, L. P. Le, G. M. Luke, B. J. Sternlieb, Y. J. Uemura, J. H. Brewer, R. Kadono, R. F. Kieff, S. R. Kreitzman, and T. M. Riseman, *Phys. Rev. B* **42**, 6801 (1990).

<sup>4</sup>J. J. Neumeier, T. Bjland, M. B. Maple, and I. K. Schuller, *Phys. Rev. Lett.* **63**, 2516 (1989).

<sup>5</sup>G. Xiao, M. Z. Cieplak, A. Gavrin, F. H. Streitz, A. Bakhshai, and C. L. Chein, *Phys. Rev. Lett.* **60**, 1446 (1988).

<sup>6</sup>K. Westerholt, H. J. Wüller, H. Bach, and P. Stauche, *Phys. Rev. B* **39**, 11 680 (1989); see also H. Alloul, P. Mendels, H. Casalta, J. F. Marucco, and J. Arabski, *Phys. Rev. Lett.* **67**, 3140 (1991).

<sup>7</sup>J. M. Tarascon, P. Barboux, P. F. Miceli, L. H. Greene, G. W. Hull, M. Eibschutz, and S. A. Sunshine, *Phys. Rev. B* **37**, 7458 (1988); N. C. Mishra, A. K. Rajarajan, K. Patnaik, R. Vijayaraghavan, and L. C. Gupta, *Solid State Commun.* **75**, 987 (1990).

<sup>8</sup>R. S. Howland, T. H. Geballe, S. S. Laderman, A. Fischer-Colbrie, M. Scott, J. M. Tarascon, and P. Barboux, *Phys. Rev. B* **39**, 9017 (1989).

<sup>9</sup>Tsuyoshi Kajitani, Keiji Kusaba, Masae Kikuchi, Yasuhiko Syono, and Makoto Hirabayashi, *Jpn. J. Appl. Phys.* **27**, L354 (1988).

<sup>10</sup>For an introduction to this phase problem, see Chap. 9 of B. E. Warren, *X-Ray Diffraction* (Dover Publications, New York, 1990).

<sup>11</sup>D. W. Green, V. M. Ingram, and M. F. Perutz, *Proc. R. Soc. London* **225**, 287 (1954); see also John R. Helliwell *Macromolecular Crystallography with Synchrotron Radiation* (Cambridge University Press, Cambridge, 1992).

<sup>12</sup>For an overview of multiwavelength anomalous diffraction (MAD), see Chap. 7 of R. Fourme and W. Hendrickson, in *Synchrotron Radiation and Biophysics*, edited by S. S. Hasnain (Ellis Horwood Limited, Chichester, 1990).

<sup>13</sup>B. W. Batterman and H. Cole, *Rev. Mod. Phys.* **36**, 681 (1964).

<sup>14</sup>B. W. Batterman, *Phys. Rev.* **133**, A759 (1964).

<sup>15</sup>J. A. Golovchenko, B. W. Batterman, and W. L. Brown, *Phys. Rev. B* **10**, 4239 (1974).

<sup>16</sup>M. J. Bedzyk and G. Materlik, *Phys. Rev. B* **32**, 6456 (1985).

<sup>17</sup>H. Mark and L. Szilard, *Z. Phys.* **33**, 688 (1925); D. Coster, K. S. Knol, and J. S. Prins, *ibid.* **63**, 345 (1930); I. G. Geib and K. Lark-Horowitz, *Phys. Rev.* **42**, 908 (1932); J. M. Bijvoet, *Proc. Acad. Sci. (Amsterdam)* **52**, 313 (1949); J. Karle, *Int. J. Quantum Chem.* **7**, 356 (1980).

<sup>18</sup>R. W. James, *The Optical Principles of the Diffraction of X-Rays* (Ox Bow Press, Woodbridge, CT, 1982).

<sup>19</sup>Dispersion corrections to the atomic scattering factors were calculated with the computer program FPRIME, supplied by D. T. Cromer, Los Alamos National Laboratory, Los Alamos, NM 87545.

<sup>20</sup>For example, see *X-ray Absorption: Principles, Applica-*

*tions, Techniques of EXAFS, SEXAFS and XANES*, edited by R. Prins and D. Koningsberger (Wiley, New York, 1988).

<sup>21</sup>R. de L. Kronig, *J. Opt. Soc. Am. Rev. Sci. Instrum.* **12**, 547 (1926).

<sup>22</sup>D. T. Cromer and D. Liberman, *J. Chem. Phys.* **53**, 1891 (1970).

<sup>23</sup>S. A. Hoffman, Ph.D. thesis, Purdue University 1991.

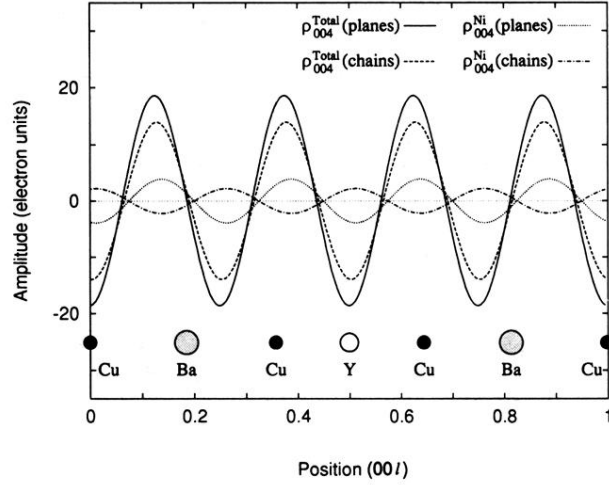


FIG. 1. The dependence of the 004 Fourier component of the scattering density function  $\rho(\mathbf{r}, E)$  on the Ni-dopant-site preference in a unit cell of  $\text{YBa}_2[\text{Cu}_{0.83}\text{Ni}_{0.17}]_3\text{O}_{7-\delta}$ . The largest sine wave (solid line) is the real part of  $\rho_{004}^{\text{total}}(\mathbf{r}, E)$  (see text) plotted against the  $c$ -axis coordinate, assuming all of the Ni dopants reside in Cu planes sites and with x rays at exactly the Ni  $K$  absorption edge energy. The large dashed-line sine curve is the corresponding  $\text{Re}[\rho_{004}^{\text{total}}(\mathbf{r}, E)]$  for Ni ions located in the Cu chain sites. The smaller dotted-line sine curve is the contribution from just the Ni ions to the generalized density function, i.e.,  $\text{Re}[\rho_{004}^{\text{Ni}}(\mathbf{r}, E)]$ , for Ni ions in the planes, and the dot-dashed sine curve is the contribution from these Ni ions in the chain sites. Also shown is the projection onto the  $c$  axis of the positions of the host structure metal ions. Note that the Cu chain site is essentially out of phase with the two Cu planes sites, and that the contributions from the Ni ions in the chains and planes have opposite signs. Also note that the relatively small amplitude (less than 20 electrons per unit cell) indicates that the 004 is a rather weak reflection, an important factor for having good sensitivity to low dopant concentrations.